



Coumarin dyes containing low-band-gap chromophores for dye-sensitised solar cells

Kang Deuk Seo^a, Hae Min Song^a, Myung Jun Lee^a, Mariachiara Pastore^b, Chiara Anselmi^b, Filippo De Angelis^b, Mohammad K. Nazeeruddin^c, Michael Grätzel^c, Hwan Kyu Kim^{a,*}

^aDepartment of Advanced Materials Chemistry & Centre for Advanced Photovoltaic Materials (ITRC), Korea University, 208 Seochang Jochiwon, Jochiwon, Chungnam 339-700, Republic of Korea

^bIstituto CNR di Scienze e Tecnologie Molecolari c/o Dipartimento di Chimica Università di Perugia, via Elce di Sotto 8, I-06123, Perugia, Italy

^cLaboratory for Photonics and Interfaces, Institute of Chemical Sciences and Engineering, Ecole Polytechnique Federale de Lausanne, 1015 Lausanne, Switzerland

ARTICLE INFO

Article history:

Received 17 November 2010

Received in revised form

18 January 2011

Accepted 19 January 2011

Available online 27 January 2011

Keywords:

Coumarin

Dye-sensitised solar cell

Low-band-gap chromophore

Ethylenedioxythiophene

Molecular orbitals

ABSTRACT

A series of coumarin dyes containing a low-band-gap chromophore of ethylenedioxythiophene (EDOT), which comprises a coumarin moiety as the electron donor and a cyanoacrylic acid moiety as electron acceptor in D- π -A chromophores, were developed for use in dye-sensitised solar cells (DSSCs). These coumarin dyes have been used to fabricate DSSCs using $\Gamma^{-}/\text{I}_3^{-}$ liquid electrolytes and their device performances were compared with that of **NKX-2677** as a standard dye. Even though **HKK-CM2** and **HKK-CM3** have more extended aromatic units than **HKK-CM1**, the degree of π -conjugation in **HKK-CM2** and **HKK-CM3** is less efficient than that of **HKK-CM1**, due to the relatively larger torsion angle between the plane of the donor and that of the acceptor. It is also in a good agreement with Density Functional Theory (DFT) calculations. As a result, a solar cell based on **HKK-CM1** sensitizer shows better photovoltaic performance with J_{SC} of 14.2 mA cm⁻², V_{OC} of 0.60 V, and a fill factor of 0.70, corresponding to an overall conversion efficiency η of 6.07% under the standard AM 1.5 irradiation, than **HKK-CM2** and **HKK-CM3**-based solar cells.

© 2011 Elsevier Ltd. All rights reserved.

1. Introduction

Dye-sensitised solar cells (DSSCs) based on mesoporous nanocrystalline TiO₂ films have attracted significant attention due to their low cost and high sunlight-to-electric power-conversion efficiencies of 10–11% [1–4]. In these cells, the sensitizer is one of the key components for high power-conversion efficiency, and the Ru(II) complex is the most efficient heterogeneous charge-transfer sensitizer that is widely used in the nanocrystalline TiO₂-based DSSC [5–9]. However, the main drawback of the Ru(II) complex sensitizer is expensive ruthenium metal and requires careful synthesis and tricky purification steps [10].

In recent years, much interest in metal-free organic dyes as an alternative to noble metal complexes has increased due to many advantages, such as diversity of molecular structures, high molar extinction coefficient, simple synthesis as well as low cost and environmental issues. Metal-free organic dyes such as triarylamine dyes [11–16], hemicyanine dyes [17,18], thiophene-based dyes [19], indoline dyes [20–26], heteropolycyclic dyes [27], porphyrin dyes

[28–31], and phthalocyanine [32] dyes, have been developed, and solar-to-electric power-conversion efficiencies have been sharply increasing reaching ca. 10% [3,33,34]. Although remarkable progress has been made in the organic dyes as sensitizers for DSSCs, it is still needed to optimise their chemical structures for further improvement in performances.

Among the metal-free organic dyes studied in DSSCs, coumarin-based dyes are still for TiO₂ kind of promising sensitizers because of their good photoresponse in the visible region, good long-term stability under one sun soaking [35], and appropriate lowest unoccupied molecular orbital (LUMO) levels matching the conduction band of TiO₂. **NKX-2677** dye has been used successfully as a photosensitizer in DSSC, and obtained maximum η value of up to 7.4% [36]. Though low-band-gap chromophore-based polymers [37–42] have been widely employed in photovoltaic applications, coumarin dyes containing low-band-gap chromophore as structural motifs have not been exploited for DSSCs. Here, we report coumarin dyes containing a low-band-gap chromophore, so-called, 3,4-ethylenedioxythiophene (EDOT) substituted coumarin derivatives, in which an electron-rich EDOT unit is connected to a donor group in order to destabilise the energy of the highest occupied molecular orbital (HOMO) in D- π -A chromophores [34,43].

* Corresponding author. Tel.: +82 41 860 1493; fax: +82 41 867 5396.
E-mail address: hkk777@korea.ac.kr (H.K. Kim).

2. Experimental

2.1. Materials

All reactions were carried out under a nitrogen atmosphere. Solvents were distilled from appropriate reagents. All reagents were purchased from Aldrich. 9-(5-bromothiophen-2-yl)-1,1,6,6-tetramethyl-2,3,5,6-tetrahydro-1H,4H,11-oxa-3a-azabenz[de]anthracen-10-one [36], 2-tri-butylstannyl-3,4-ethyl-enedioxythiophene [44], 2-tributylstannyl-5-dioxolanylthiophene [45] were synthesised by following the same procedures as described previously.

2.2. Measurement

The ^1H NMR spectra were recorded at room temperature with Varian Oxford 300 spectrometers and chemical shifts were reported in ppm units with tetramethylsilane as an internal standard. FT-IR spectra were measured as KBr pellets on a Perkin Elmer Spectrometer. UV–visible absorption spectra were obtained in THF on a Shimadzu UV-2401PC spectrophotometer. Cyclic voltammetry was carried out with a Versa STAT3 (AMETEK). A three-electrode system was used and consisted of a reference electrode (Ag/AgCl), a working electrode, and a platinum wire electrode. Redox potential of dyes on TiO_2 was measured in CH_3CN with 0.1 M TBAPF₆ with a scan rate between 50 mV s⁻¹.

2.3. Density functional theory (DFT)/time-dependent DFT (TDDFT) calculations

The ground state geometries of the dyes have been optimised, in gas phase, by DFT employing the B3LYP [46] functional and a 6-31G* basis set; only the protonated species have been considered. The vertical excitation energies in THF have been calculated by TDDFT at MPW1K [47]/6-31G* level, including the solvation effects by the Conductor-like Polarizable Continuum Model (CPCM) [48]. All the calculations were carried out with GAUSSIAN 03 [49].

2.4. Synthesis

2.4.1. Preparation of 5-((1,1,6,6-tetramethyl-10-oxo-2,3,5,6-tetrahydro-1H,4H,10H-11-oxa-3a-azabenz[de]anthracen-9-yl)-thiophene-2-yl)-3,4-ethylenedioxythiophene (3)

A mixture of compound 1 (4.00 g, 8.73 mmol), compound 2 (4.90 g, 11.4 mmol) and Pd(PPh₃)₄ (0.80 g, 0.69 mmol) was heated in dry THF 250 mL at 80 °C for 20 h under an inert N₂ atmosphere. After concentration, the residue was dissolved in CH_2Cl_2 . The organic phase was washed twice with a saturated solution of NaHCO₃ and then with water. After drying over MgSO₄ and evaporating the solvent, the product was purified by chromatography on silica gel (CH_2Cl_2 –hexane 2:1) to give compound 3 as an orange solid. Yield was 59%. ^1H NMR (300 MHz, CDCl_3) δ (TMS, ppm): 1.31 (6H, s), 1.56 (6H, s), 1.76–1.83 (4H, m), 3.22–3.33 (4H, m), 4.25–4.34 (4H, m), 6.22 (1H, s), 7.14 (1H, s), 7.19 (1H, d), 7.61 (1H, d), 7.81 (1H, s).

2.4.2. Preparation of 5-((1,1,6,6-tetramethyl-10-oxo-2,3,5,6-tetrahydro-1H,4H,10H-11-oxa-3a-azabenz[de]anthracen-9-yl)-thiophene-2-yl)-3,4-ethylenedioxythiophene carbaldehyde (4)

Compound 3 (0.42 g, 0.81 mmol) was dissolved in 10 mL of DMF and then phosphorus oxychloride (0.21 g, 1.37 mmol) was added into the solution, which was then kept at room temperature for 1.5 h. The resulting solution was added to water. After neutralisation with 25% (wt/wt) NaOH solution, the solution was kept at 50 °C

for 0.5 h. The mixture was extracted with chloroform and then washed with aqueous saturated NaCl solution and then dried over MgSO₄. After filtration and evaporation of the solvent, the resulting precipitate was recrystallised from DMF. Yield was 59%. ^1H NMR (300 MHz, CDCl_3) δ (TMS, ppm): 1.32 (6H, s), 1.58 (6H, s), 1.75–1.84 (4H, m), 3.25–3.33 (4H, m), 4.43 (4H, s), 7.16 (1H, s), 7.41 (1H, d), 7.60 (1H, d), 7.88 (1H, s), 9.89 (1H, s).

2.4.3. Preparation of 5-((1,1,6,6-tetramethyl-10-oxo-2,3,5,6-tetrahydro-1H,4H,10H-11-oxa-3a-azabenz[de]anthracen-9-yl)-thiophene-2-yl)-3,4-ethylenedioxythiophene-5-yl) acrylic acid (HKK-CM1)

An acetonitrile solution (15 mL) of compound 4 (0.25 g, 0.46 mmol) and cyanoacetic acid (0.07 g, 0.82 mmol) was refluxed at 120 °C in the presence of piperidine (0.04 mL) for 6 h. After cooling the solution, the product was purified by chromatography on silica gel (CH_2Cl_2 –MeOH 5:1). Yield was 69%. ^1H NMR (DMSO-d₆) δ (TMS, ppm): 1.27 (6H, s), 1.48 (6H, s), 1.70–1.76 (4H, m), 3.27–3.33 (4H, m), 4.53 (4H, s), 7.40 (1H, s), 7.44 (1H, d), 7.66 (1H, d), 8.07 (1H, s), 8.38 (1H, s). UV–vis (THF, nm): λ_{max} (log ϵ) 532 (52,700). PL (THF, nm): λ_{max} 666. FAB-mass: Calcd. for C₃₃H₃₀N₂O₆S₂, 614.15; found, 614.00.

2.4.4. Preparation of 5-((1,1,6,6-tetramethyl-10-oxo-2,3,5,6-tetrahydro-1H,4H,10H-11-oxa-3a-azabenz[de]anthracen-9-yl)-thiophene-2-yl)-5-bromo-3,4-ethylenedioxythiophene (5)

Compound 3 (1.74 g, 3.35 mmol) was dissolved in 20 mL of DMF and then 13 mL of DMF solution including N-bromosuccinimide (0.18 g, 3.43 mmol) was added to the solution, which was then kept for 12 h. Ethanol (60 mL) and water (10 mL) were added and a precipitate of compound 6 was formed. Yield was 56%. ^1H NMR (300 MHz, CDCl_3) δ (TMS, ppm): 1.31 (6H, s), 1.57 (6H, s), 1.74–1.83 (4H, m), 3.22–3.30 (4H, m), 4.25–4.34 (4H, m), 7.11 (1H, s), 7.13 (1H, d), 7.61 (1H, d), 7.81 (1H, s).

2.4.5. Preparation of 5-((1,1,6,6-tetramethyl-10-oxo-2,3,5,6-tetrahydro-1H,4H,10H-11-oxa-3a-azabenz[de]anthracen-9-yl)-thiophene-2-yl)-3,4-ethylenedioxythiophenyl-5-benzaldehyde (6)

Compound 5 (0.57 g, 0.94 mmol), 4-formyl phenyl boronic acid (0.17 g, 1.13 mmol), Pd(PPh₃)₄ (0.07 g, 0.06 mmol), Na₂CO₃ (0.40 g, 3.77 mmol) in H₂O were dissolved in 40 mL of solvent (THF and toluene, 1:1) and then kept at 80 °C for 8 h under an inert N₂ atmosphere. The mixture was extracted with chloroform and then washed with aqueous saturated NaCl solution and then dried over dehydrated MgSO₄. After filtration and evaporation of the solvent, the resulting precipitate was recrystallised from DMF. Yield was 88%. ^1H NMR (300 MHz, CDCl_3) δ (TMS, ppm): 1.32 (6H, s), 1.58 (6H, s), 1.77–1.82 (4H, m), 3.24–3.31 (4H, m), 4.43 (4H, s), 7.15 (1H, s), 7.26 (1H, d), 7.61 (1H, d), 7.84–7.90 (5H, m), 9.96 (1H, s).

2.4.6. Preparation of 5-(((1,1,6,6-tetramethyl-10-oxo-2,3,5,6-tetrahydro-1H,4H,10H-11-oxa-3a-azabenz[de]anthracen-9-yl)-thiophene-2-yl)-3,4-ethylenedioxythiophene-5-yl)-benzyl-4-yl) acrylic acid (HKK-CM2)

An acetonitrile solution (15 mL) of compound 6 (0.51 g, 0.82 mmol) and cyanoacetic acid (0.11 g, 1.29 mmol) was refluxed at 120 °C in the presence of piperidine (0.07 mL) for 6 h. After cooling the solution, the product was purified by chromatography on silica gel (CH_2Cl_2 –MeOH 5:1). Yield was 69%. ^1H NMR (DMSO-d₆) δ (TMS, ppm): 1.27 (6H, s), 1.58 (6H, s), 1.70–1.78 (4H, m), 3.26–3.33 (4H, m), 4.43 (4H, s), 7.33 (1H, d), 7.42 (1H, s), 7.64 (1H, d), 7.83 (2H, d), 8.03 (2H, d), 8.22 (1H, s), 8.32 (1H, s). UV–vis (THF, nm): λ_{max} (log ϵ) 509 (67,200). PL (THF, nm): λ_{max} 597. FAB-mass: Calcd. for C₃₉H₃₄N₂O₆S₂, 690.19; found, 690.00.

2.4.7. Preparation of 5-(((1,1,6,6-tetramethyl-10-oxo-2,3,5,6-tetrahydro-1H,4H,10H-11-oxa-3a-azabenzode[de]anthracen-9-yl)-thiophene-2-yl)-3,4-ethylenedioxythiophenyl-5-thiophenylaldehyde (8)

A mixture of compound 5 (0.54 g, 0.91 mmol), compound 7 (0.60 g, 1.35 mmol) and Pd(PPh₃)₄ (0.08 g, 0.07 mmol) was heated in dry THF 100 mL at 80 °C for 24 h under an inert N₂ atmosphere. After concentration, the residue was dissolved in CH₂Cl₂. The organic phase was washed twice with a saturated solution of NaHCO₃ and then with water. After drying over MgSO₄ and evaporating the solvent, the product was suspended in glacial acetic acid (25 mL) and heated at 50 °C for 5 h. The mixture was cooled and added to ice water. The resulting orange precipitate formed was filtered and washed with water and methanol. The compound 10 was recrystallised from DMF. Yield was 52%. ¹H NMR (300 MHz, CDCl₃) δ (TMS, ppm): 1.32 (6H, s), 1.58 (6H, s), 1.77–1.82 (4H, m), 3.24–3.32 (4H, m), 4.43 (4H, s), 7.15 (1H, s), 7.23–7.28 (2H, m), 7.60–7.67 (2H, m), 7.84 (1H, s), 9.84 (1H, s).

2.4.8. Preparation of 5-(((1,1,6,6-tetramethyl-10-oxo-2,3,5,6-tetrahydro-1H,4H,10H-11-oxa-3a-azabenzode[de]anthracen-9-yl)-thiophene-2-yl)-3,4-ethylenedioxythiophene-5-yl)-thiophene-2-yl) acrylic acid (HKK-CM3)

An acetonitrile solution (20 mL) of compound 8 (0.30 g, 0.48 mmol) and cyanoacetic acid (0.07 g, 0.76 mmol) was refluxed at 120 °C in the presence of piperidine (0.05 mL) for 6 h. After cooling the solution, the product was purified by chromatography on silica gel (CH₂Cl₂–MeOH 5:1). Yield was 76%. ¹H NMR (DMSO-d₆) δ (TMS, ppm): 1.26 (6H, s), 1.49 (6H, s), 1.70–1.77 (4H, m), 3.26–3.32 (4H, m), 4.54 (4H, s), 7.33 (1H, s), 7.37 (1H, d), 7.40 (1H, s), 7.69 (1H, d), 7.88 (1H, d), 8.31 (1H, s), 8.37 (1H, s), 7.33 (1H, d), 7.42 (1H, s), 7.64 (1H, d), 7.83 (2H, d), 8.03 (2H, d), 8.22 (1H, s), 8.32 (1H, s). UV–vis (THF, nm): λ_{max} (log ε) 527 (60,400). PL (THF, nm): λ_{max} 620. FAB-mass: Calcd. for C₃₇H₃₂N₂O₆S₃, 696.14; found, 696.00.

2.5. Fabrication and testing of DSSC

FTO glass plates (Pilkington) were cleaned in a detergent solution using an ultrasonic bath for 1 h, rinsed with water and ethanol. The FTO glass plates were immersed in an aqueous solution of 40 mM TiCl₄ at 70 °C for 30 min and washed with water and ethanol. The first TiO₂ layer of 8 μm thickness was prepared by screen printing TiO₂ paste (Solaronix, 13 nm anatase), and the second scattering layer containing 400 nm sized anatase particles was deposited by screen printing. The TiO₂ electrodes were immersed into the dye solution (0.3 mM in ethanol/THF (1:1) with DCA (10 mM)) and kept at room temperature overnight. Counter electrodes were prepared by coating with a drop of H₂PtCl₆ solution (2 mg of Pt in 1 mL of ethanol) on an FTO plate. The dye-adsorbed TiO₂ electrode and Pt-counter electrode were assembled into a sealed sandwich-type cell. A drop of electrolyte was then introduced into the cell, which was composed of 0.6 M 1,2-dimethyl-3-propyl imidazolium iodide, 0.05 M iodine, 0.1 M LiI, and 0.5 M tert-butylpyridine in acetonitrile. It was introduced into the inter-electrode space from the counter electrode side through predrilled holes. The drilled holes were sealed with a microscope cover slide and Surlyn to avoid leakage of the electrolyte solution.

2.6. Photoelectrochemical measurements of DSSC

Photoelectrochemical data were measured using a 1000 W xenon light source (Oriol, 91193) that was focused to give 1000 W m², the equivalent of one sun at Air Mass (AM) 1.5, at the surface of the test cell. The light intensity was adjusted with a Si solar cell that was double-checked with an NREL-calibrated Si solar

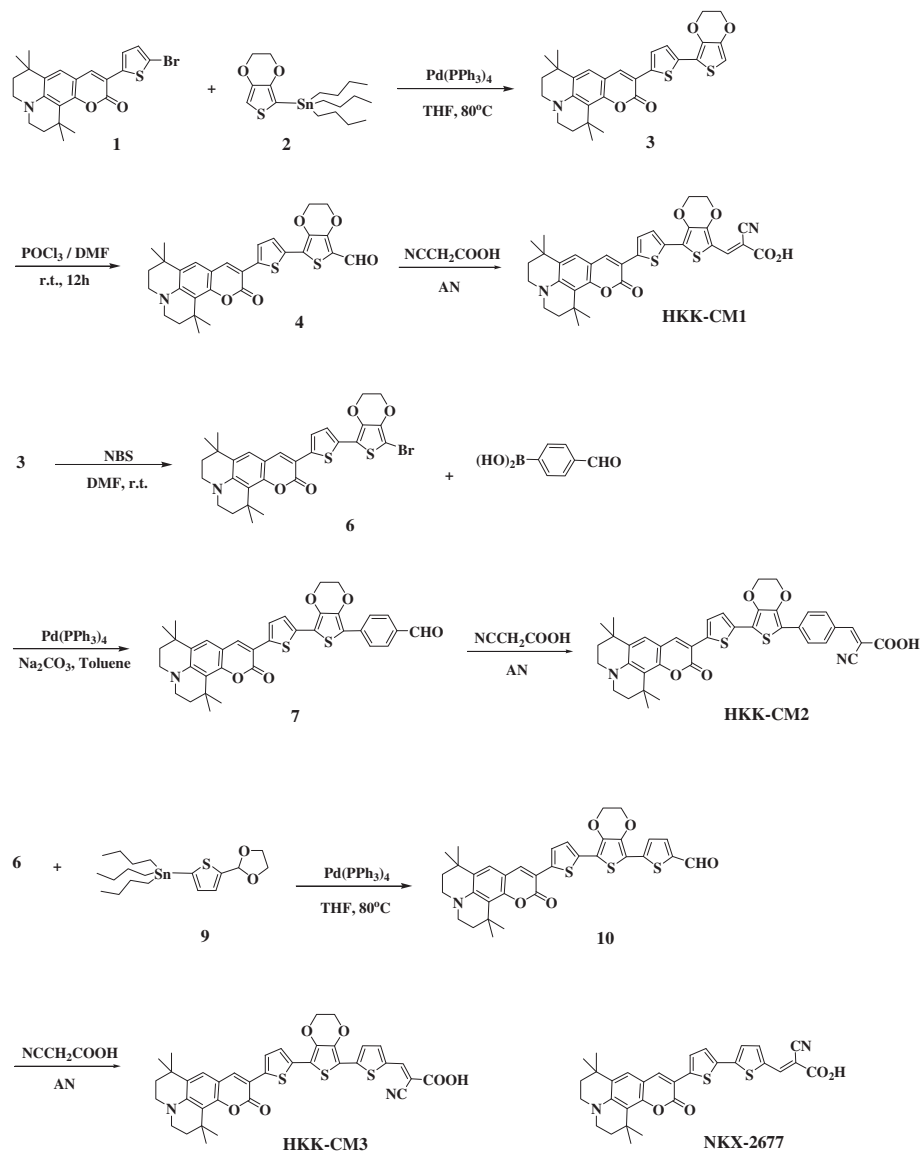
cell (PV Measurement Inc.). The applied potential and measured cell current were measured using a Keithley model 2400 digital source metre. The current–voltage characteristics of the cell under these conditions were determined by biasing the cell externally and measuring the generated photocurrent. This process was fully automated using Wavemetrics software.

3. Results and discussion

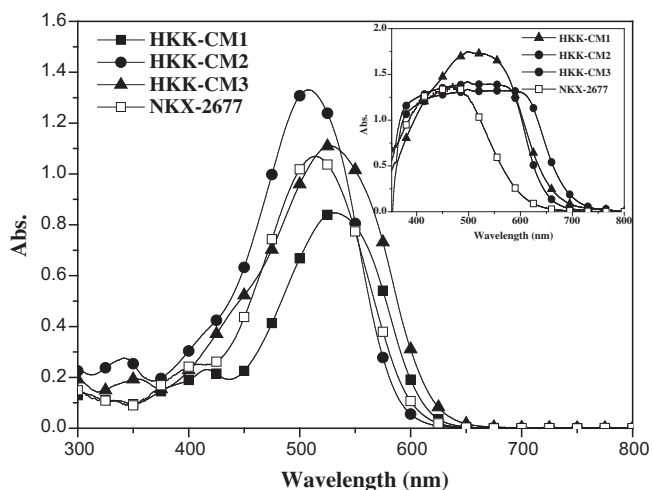
The synthetic procedures of the coumarin dyes containing EDOT are depicted in Scheme 1. Coumarin aldehyde derivatives were synthesized by either a Suzuki or Stille coupling reaction. These aldehydes, on reaction with cyanoacetic acid in the presence of piperidine catalyst, produced a series of coumarin dyes of **HKK-CM1-3**, presented here.

Fig. 1 shows the absorption and emission spectra of coumarin dyes measured in THF solution and their photophysical properties are summarised in Table 1. The calculated TDDFT absorption wavelengths, together with the corresponding oscillator strengths, are reported in Table 2. The absorption spectrum of the **HKK-CM1** dye with the incorporation of an EDOT unit into a bithiophene-containing coumarin dye of **NKX-2677** to up-lift its HOMO level and down-shift its LUMO level, shows the maximum absorption of 532 nm (ε = 52,700 M⁻¹ cm⁻¹), which is 18 nm red-shifted in contrast to **NKX-2677**. In excellent agreement with experiment, a small red shift is also predicted by TDDFT with λ_{max} of 519 (**HKK-CM1**) and 513 (**NKX-2677**) nm. Under a similar condition, the **HKK-CM3** dye exhibits the maximum absorption peak at 527 nm (ε = 60,400 M⁻¹ cm⁻¹). Obviously, with the introduction of the EDOT, the charge-transfer transition absorption is not only red-shifted but also its absorption molar extinction coefficient is enhanced, due to extended π-conjugation. As shown in Table 2, for **HKK-CM3**, the first absorption maximum is computed at 543 nm with a larger oscillator strength (2.202) with respect to those of **HKK-CM1** (1.839) and **NKX-2677** (1.857). But, the **HKK-CM2** dye exhibits the maximum absorption peak at 509 nm (ε = 67,200 M⁻¹ cm⁻¹), which is 5 nm blue-shifted in contrast to **NKX-2677**; a comparable shift to shorter wavelengths is also computed by TDDFT, which locates the first absorption band at 511 nm with an oscillator strength of 2.268. This increase in the excitation energy of **HKK-CM2** can be ascribed to the relatively larger torsion angle (ca. 9° at B3LYP/6-31G* level) between the plane of the donor and that of the acceptor, induced by the presence of the phenyl fragment, ensuring less efficient electronic communication between the donor and the acceptor. In contrast, the absorption spectra of coumarin dyes adsorbed on the TiO₂ surface are remarkably broadened relative to the absorption spectra of the solution state. This might be due to dye–dye and/or dye–TiO₂ interactions [50]. In addition, it should be addressed that a series of coumarin dyes of **HKK-CM1-3** adsorbed on the TiO₂ films has a broader and better absorption band than that of **NKX-2677** as a standard dye.

The electrochemical properties were investigated by cyclic voltammetry (CV) to obtain HOMO and LUMO levels of the present dyes. The cyclic voltammogram curves were obtained from a three-electrode cell in 0.1 M TBAPF₆ in CH₃CN at the scan rate of 50 mV/s, using a dye-coated TiO₂ electrode as a working electrode and Pt wire counter electrode and Ag/AgCl (saturated KCl) reference electrode (+0.197 V vs NHE) and calibrated with ferrocene. All of the measured potentials were converted to the NHE scale. The band gap was estimated from the absorption edges of UV–vis spectra and LUMO energy levels were derived from HOMO energy levels and the band gap. HOMO values (0.93–1.02 V vs NHE) are more positive than the I⁻/I₃⁻ redox couple (0.4 V vs NHE). The electron injection from the excited sensitizers to the conduction band of



Scheme 1. Chemical structures and synthesis of coumarin dyes containing EDOT.

Fig. 1. Absorption and emission spectra of 2×10^{-5} M coumarin dyes in THF (inset: dyes adsorbed on TiO_2 films).

TiO_2 should be energetically favourable because of the more negative LUMO values (-1.13 to -1.24 vs NHE) compared to the conduction band edge energy level of the TiO_2 electrode [51]. As shown in Fig. 3, **HKK-CM1** only exhibits the lifted HOMO level, since it is well known that an EDOT electron-rich EDOT unit is

Table 1
Optical properties and DSSC performance parameters of coumarin dyes.

Dye	$\lambda_{\text{abs}}^a/\text{nm}$ ($\epsilon/\text{M}^{-1}\text{cm}^{-1}$)	E_{ox}^b/V	E_{0-0}^c/eV	$E_{\text{LUMO}}^d/\text{V}$	J_{sc} (mA cm^{-2})	V_{oc} (eV)	FF	η (%)
HKK-CM1	532 (52,700)	0.93	2.06	-1.13	14.2	0.60	0.70	6.07
HKK-CM2	509 (67,200)	0.99	2.23	-1.24	10.5	0.62	0.57	3.73
HKK-CM3	527 (60,400)	1.02	2.15	-1.13	13.3	0.57	0.56	4.37
NKX-2677	514 (59,900)	0.95	2.17	-1.18	16.1	0.64	0.70	7.19

^a Absorption and emission spectra were measured in THF.

^b Oxidation potentials of dyes on TiO_2 were measured in CH_3CN with 0.1 M TBAPF₆ with a scan rate of 50 mV s^{-1} (vs NHE).

^c E_{0-0} was determined from the intersection of absorption and emission spectra in THF.

^d LUMO was calculated by $E_{\text{ox}} - E_{0-0}$.

Table 2
Computed and experimental maximum absorption wavelengths (λ_{\max}) and oscillator strengths in THF for **HKK-CM1**, **HKK-CM2**, **HKK-CM3** and **NKX-2677**.

Dye	λ_{\max} (nm) (Exp.)	λ_{\max} (nm) (Theor.)	$\epsilon/M^{-1} \text{ cm}^{-1}$ (Exp.)	Osc. Strength (Theor.)
HKK-CM1	532	519	52,700	1.839
HKK-CM2	509	511	67,200	2.268
HKK-CM3	527	543	60,400	2.202
NKX-2677	514	513	59,900	1.857

connected to donor group in D- π -A chromophores and destabilised the energy of the HOMO to be lifted [34,43]. In contrast, it was surprising that **HKK-CM2** and **HKK-CM3** exhibit the lowered HOMO level. To gain more insight of their photophysical behaviour adsorbed on TiO₂ films, theoretical analysis (DFT, B3LYP/6-31G* level) on the molecular orbitals involved in the transitions was carried out, and the resulting frontier orbitals are depicted in further density functional B3LYP/3-21G* calculations performed for three compounds. Fig. 2 shows the dominant electron density change for the HOMO-LUMO transition is that the electrons transfer from the coumarin unit to acrylic acid moiety in D- π -A chromophores.

Fig. 4 shows the incident monochromatic photon-to-current conversion efficiency (IPCE) of the coumarin dyes sensitised. The onset wavelengths of the IPCE spectra for DSSCs based on **HKK-CM2** and **HKK-CM3** were >800 nm. IPCE values of higher than 70% were observed in the range of 410–605 nm with a maximum value of 78% at 500 nm for the DSSC based on **HKK-CM1**. The maximum IPCE value of the DSSC based on **HKK-CM2** and **HKK-CM3** are slightly lower than the efficiencies of the DSSCs based on **HKK-CM1**.

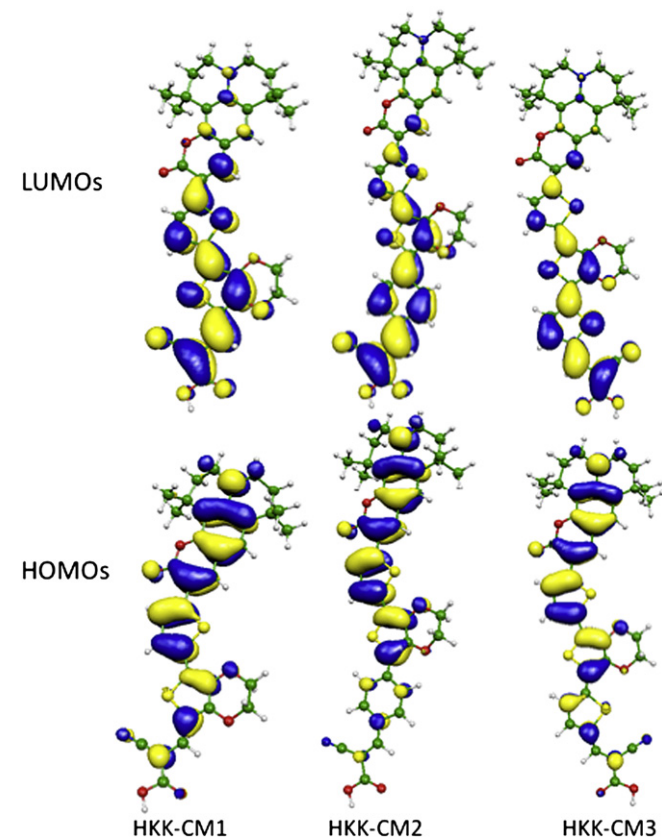


Fig. 2. Plots of the isodensity surfaces (MPW1K/6-31G* in THF) of HOMOs and LUMOs of **HKK-CM1**, **HKK-CM2** and **HKK-CM3**.

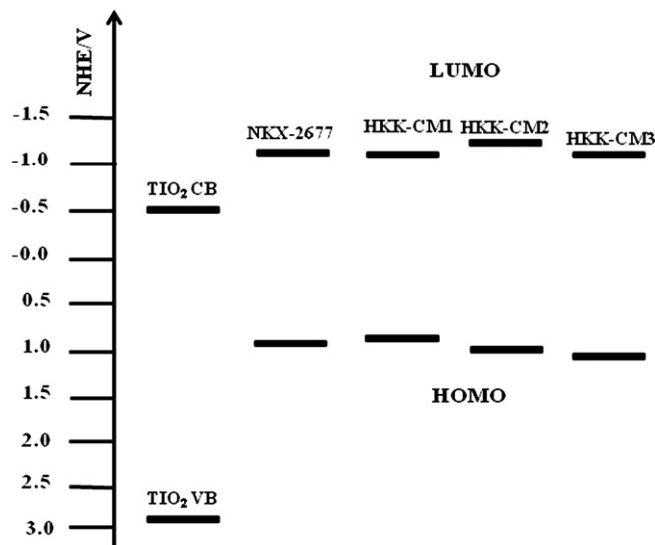


Fig. 3. Overview of the evaluated energy levels of coumarin dyes determined by cyclic voltammetry.

But, all maximum IPCE values of the DSSC based on the presented coumarin dyes are lower than that of the DSSCs based on **NKX-2677**, even though a series of coumarin dyes of **HKK-CM1-3** adsorbed on the TiO₂ films has a broader and better absorption band than that of **NKX-2677** as a standard dye (see Fig. 1). The lower IPCE values of the DSSC based on **HKK-CM2** and **HKK-CM3** are probably due to extended π -conjugation elongation, which might lead to decreased electron-injection yield relative to that of **HKK-CM1** dye [36].

The photovoltaic performances of the coumarin DSSCs were summarised in Table 1. Under the standard global AM 1.5 solar condition, the **HKK-CM1** sensitised cell gave a short circuit photocurrent density (J_{SC}) of 14.2 mA cm⁻², open circuit voltage (V_{OC}) of 0.60 V, and a fill factor (FF) of 0.70, corresponding to an overall conversion efficiency of 6.07%. The **HKK-CM2** sensitised cell gave a J_{SC} of 10.5 mA cm⁻², V_{OC} of 0.62 V, and FF of 0.57, corresponding to an overall conversion efficiency η of 3.73% and the **HKK-CM3** sensitised cell gave a J_{SC} of 13.3 mA cm⁻², V_{OC} of 0.57 V, and FF of 0.56, corresponding to an overall conversion efficiency η of 4.37%. Fig. 5

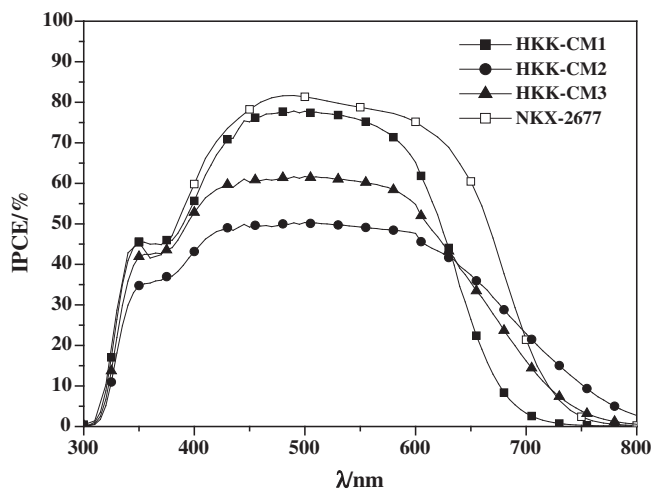


Fig. 4. Typical action spectra of incident photon-to-current conversion efficiencies (IPCE) obtained for nanocrystalline TiO₂ solar cells sensitized by coumarin dyes.

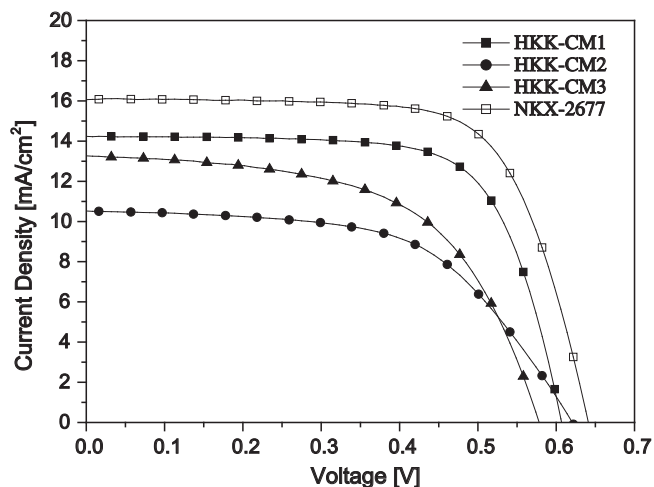


Fig. 5. Photocurrent–voltage characteristics of representative TiO_2 electrodes sensitized with coumarin dyes.

shows the J – V curves of the coumarin dyes. Among the three dye-based DSSCs, the **HKK-CM2**-based device gives the lowest efficiency although the dye gave the broadest light harvesting range. The phenylene unit in **HKK-CM2** may also lead to a twisted intramolecular charge-transfer geometry of the dye excited state, which would decrease the excited-state energy and cause a lower efficiency of electron injection as reported previously [52].

4. Conclusions

Coumarin dyes containing low-band-gap chromophore have been designed and synthesized. Surprisingly, even though **HKK-CM2** and **HKK-CM3** have more extended aromatic units than **HKK-CM1**, the degree of π -conjugation in **HKK-CM2** and **HKK-CM3** is less efficient than that of **HKK-CM1**, due to the relatively larger torsion angle between the plane of the donor and that of the acceptor. As a result, a solar cell based on **HKK-CM1** sensitizer shows better photovoltaic performance with J_{SC} of 14.2 mA cm^{-2} , V_{OC} of 0.60 V, and FF of 0.70, corresponding to an overall conversion efficiency η of 6.07% under the standard AM 1.5 irradiation, than **HKK-CM2** and **HKK-CM3**-based solar cells. The lower IPCE values of the DSSCs based on **HKK-CM2** and **HKK-CM3** are probably due to extended π -conjugation elongation, which might lead to decreased electron-injection yield relative to that of **HKK-CM1** dye.

Acknowledgements

This research was supported by MKE (The Ministry of Knowledge Economy), Korea, under the ITRC support program supervised by the IITA (Institute for Information Technology Advancement) (IITA-2008-C1090-0804-0013), WCU (the Ministry of Education and Science) program (R31-2008-000-10035-0) and Converging Research Center Program through the Ministry of Education, Science and Technology (2010K000973).

Appendix. Supplementary material

Supplementary data related to this article can be found online at doi:10.1016/j.dyepig.2011.01.009.

References

[1] Nazeeruddin MK, De Angelis F, Fantacci S, Selloni A, Viscardi G, Grätzel M, et al. Combined experimental and DFT-TDDFT computational study of

photoelectrochemical cell ruthenium sensitizers. *J Am Chem Soc* 2005;127:16835–47.

[2] Nazeeruddin MK, Pechy P, Renouard T, Zakeeruddin SM, Humphry-Baker R, Grätzel M, et al. Engineering of efficient panchromatic sensitizers for nanocrystalline TiO_2 -based solar cells. *J Am Chem Soc* 2001;123:1613–24.

[3] Mishra A, Fischer MKR, Bäuerle P. Metal-free organic dyes for dye-sensitized solar cells: from structure: property relationships to design rules. *Angew Chem Int Ed* 2009;48:2474–99.

[4] Ning Z, Fu Y, Tian H. Improvement of dye-sensitized solar cells: what we know and what we need to know. *Energy Environ Sci* 2010;3:1170–81.

[5] Asbury JB, Ellingson RJ, Gosh HN, Ferrere S, Notz AJ, Lian T. Femtosecond IR study of excited-state relaxation and electron-injection dynamics of $\text{Ru}(\text{dcbpy})_2(\text{NCS})_2$ in solution and on nanocrystalline TiO_2 and Al_2O_3 thin films. *J Phys Chem B* 1999;103:3110–9.

[6] Park NG, Kang MG, Kim KM, Ryu KS, Kim DK, Frank AJ, et al. Morphological and photoelectrochemical characterization of core-shell nanoparticle films for dye-sensitized solar cells: Zn–O type shell on SnO_2 and TiO_2 cores. *Langmuir* 2004;20:4246–53.

[7] Saito Y, Fukuri N, Senadeera R, Kitamura T, Wada Y, Yanagida S. Solid state dye sensitized solar cells using in situ polymerized PEDOTs as hole conductor. *Electrochem Commun* 2004;6:71–4.

[8] Fabregat-Santiago F, Garcia-Cañadas J, Palomares E, Clifford JN, Durrant JR, Bisquert J, et al. The origin of slow electron recombination processes in dye-sensitized solar cells with alumina barrier coatings. *J Appl Phys* 2004;96:6903–7.

[9] Furube A, Katoh R, Hara K, Murata S, Arakawa H, Tachiya M, et al. Ultrafast direct and indirect electron-injection processes in a photoexcited dye-sensitized nanocrystalline zinc oxide film: the importance of exciplex intermediates at the surface. *J Phys Chem B* 2004;108:12583–92.

[10] Tian H, Meng F. *Organic photovoltaics: mechanisms, materials, and devices*. London: CRC; 2005.

[11] Wu W, Yang J, Hua J, Tang J, Zhang L, Tian H, et al. Efficient and stable dye-sensitized solar cells based on phenothiazine sensitizers with thiophene units. *J Mater Chem* 2010;20:1772–9.

[12] Qu S, Wu W, Hua J, Kong C, Long Y, Tian H. New diketopyrrolopyrrole (DPP) dyes for efficient dye-sensitized solar cells. *J Phys Chem C* 2010;114:1343–9.

[13] Ning Z, Tian H. Triarylamine: a promising core unit for efficient photovoltaic materials. *Chem Commun*; 2009:5483–95.

[14] Xu W, Peng B, Chen J, Liang M, Cai F. New triphenylamine-based dyes for dye-sensitized solar cells. *J Phys Chem C* 2008;112:874–80.

[15] Ning Z, Zhang Q, Wu W, Pei H, Liu B, Tian H. Starburst triarylamine based dyes for efficient dye-sensitized solar cells. *J Org Chem* 2008;73:3791–7.

[16] Li G, Jiang KJ, Li YF, Li SL, Yang LM. Efficient structural modification of triphenylamine-based organic dyes for dye-sensitized solar cells. *J Phys Chem C* 2008;112:11591–9.

[17] Wang ZS, Li FY, Huang CH, Wang L, Wei M, Jin LP, et al. Photoelectric conversion properties of nanocrystalline TiO_2 electrodes sensitized with hemicyanine derivatives. *J Phys Chem B* 2000;104:9676–82.

[18] Chen YS, Li C, Zeng ZH, Wang WB, Wang XS, Zhang BW. Efficient electron injection due to a special adsorbing group's combination of carboxyl and hydroxyl: dye-sensitized solar cells based on new hemicyanine dyes. *J Mater Chem* 2005;15:1654–61.

[19] Tanaka K, Takimiya K, Otsubo T, Kawabuchi K, Kajihara S, Harima Y. Development and photovoltaic performance of oligothiophene-sensitized TiO_2 solar cells. *Chem Lett* 2006;35:592–3.

[20] Horiuchi T, Miura H, Uchida S. Highly efficient metal-free organic dyes for dye-sensitized solar cells. *J Photochem Photobiol Chem* 2004;164:29–32.

[21] Horiuchi T, Miura H, Sumioka K, Uchida S. High efficiency of dye-sensitized solar cells based on metal-free indoline dyes. *J Am Chem Soc* 2004;126:12218–9.

[22] Schmidt-Mende L, Bach U, Humphry-Baker R, Horiuchi T, Miura H, Ito S, et al. Organic dye for highly efficient solid-state dye-sensitized solar cells. *Adv Mater* 2005;17:813–5.

[23] Ito S, Zakeeruddin SM, Humphry-Baker R, Liska P, Charvët R, Grätzel M, et al. High-efficiency organic-dye-sensitized solar cells controlled by nanocrystalline- TiO_2 electrode thickness. *Adv Mater* 2006;18:1202–5.

[24] Howie WH, Claeysens F, Miura H, Peter ML. Characterization of solid-state dye-sensitized solar cells utilizing high absorption coefficient metal-free organic dyes. *J Am Chem Soc* 2008;130:1367–75.

[25] Kuang D, Uchida S, Humphry-Baker R, Zakeeruddin SK, Grätzel M. Organic dye-sensitized ionic liquid based solar cells: remarkable enhancement in performance through molecular design of indoline sensitizers. *Angew Chem Int Ed* 2008;47:1923–7.

[26] Ito S, Miura H, Uchida S, Takata M, Sumioka K, Liska P, et al. High-conversion-efficiency organic dye-sensitized solar cells with a novel indoline dye. *Chem Commun*; 2008:5194–6.

[27] Ooyama Y, Shimada Y, Kagawa Y, Imae I, Harima Y. Photovoltaic performance of dye-sensitized solar cells based on donor–acceptor π -conjugated benzo-furo[2,3-c]oxazolo[4,5-a]carbazole-type fluorescent dyes with a carboxyl group at different positions of the chromophore skeleton. *Org Biomol Chem* 2007;5:2046–54.

[28] Imahori H, Umeyama T, Ito S. Large π -aromatic molecules as potential sensitizers for highly efficient dye-sensitized solar cells. *Acc Chem Res* 2009;42:1809–18.

- [29] Lu HP, Tsai CY, Yen WN, Hsieh CP, Yeh CY, Diao EWG, et al. Control of dye aggregation and electron injection for highly efficient porphyrin sensitizers adsorbed on semiconductor films with varying ratios of coadsorbate. *J Phys Chem C* 2009;113:20990–7.
- [30] Imahori H, Matsubara Y, Iijima H, Umeyama T, Matano Y, Ito S, et al. Effects of *meso*-diaryl amino group of porphyrins as sensitizers in dye-sensitized solar cells on optical, electrochemical, and photovoltaic properties. *J Phys Chem C* 2010;114:10656–65.
- [31] Mai CL, Huang WK, Lu HP, Lee CW, Diao EWG, Yeh CY, et al. Synthesis and characterization of diporphyrin sensitizers for dye-sensitized solar cells. *Chem Commun* 2010;46:809–11.
- [32] Eu S, Katoh T, Umeyama T, Matano Y, Imahori H. Synthesis of sterically hindered phthalocyanines and their applications to dye-sensitized solar cells. *Dalton Trans*; 2008:5476–83.
- [33] Ooyama Y, Harima H. Molecular designs and syntheses of organic dyes for dye-sensitized solar cells. *European J Org Chem*; 2009:2903–34.
- [34] Zeng W, Cao Y, Bai Y, Wang Y, Shi Y, Wang P. Efficient dye-sensitized solar cells with an organic photosensitizer featuring orderly conjugated ethylenedioxythiophene and dithienosilole blocks. *Chem Mater* 2010;22:1915–25.
- [35] Wang ZS, Cui Y, Hara K, Dan-oh Y, Kasada C, Shinpo A. A high-light-harvesting-efficiency coumarin dye for stable dye-sensitized solar cells. *Adv Mater* 2007;19:1138–41.
- [36] Hara K, Wang ZS, Sato T, Furube A, Katoh R, Sugihara H, et al. Oligothiophene-containing coumarin dyes for efficient dye-sensitized solar cells. *J Phys Chem B* 2005;109:15476–82.
- [37] Ehret A, Stuhl L, Spitler MT. Spectral sensitization of TiO₂ nanocrystalline electrodes with aggregated cyanine dyes. *J Phys Chem B* 2001;105:9960–5.
- [38] Yao QH, Meng FS, Li FY, Tian H, Huang CH. Photoelectric conversion properties of four novel carboxylated hemicyanine dyes on TiO₂ electrode. *J Mater Chem* 2003;13:1048–53.
- [39] Wang ZS, Li FY, Huang CH. Highly efficient sensitization of nanocrystalline TiO₂ films with styryl benzothiazolium propylsulfonate. *Chem Commun*; 2000:2063–4.
- [40] Yang R, Tian R, Yan J, Zhang Y, Yang J, Cao Y, et al. Deep-red electroluminescent polymers: synthesis and characterization of new low-band-gap conjugated copolymers for light-emitting diodes and photovoltaic devices. *Macromolecules* 2005;38:244–53.
- [41] Zhang FL, Gadisa A, Inganäs O, Svensson M, Andersso MR. Influence of buffer layers on the performance of polymer solar cells. *Appl Phys Lett* 2004;84:3906–8.
- [42] Kim J, Kim SH, Jung IH, Jeong E, Xia Y, Woo HY, et al. Synthesis and characterization of indeno[1,2-*b*]fluorene-based low bandgap copolymers for photovoltaic cells. *J Mater Chem* 2010;20:1577–86.
- [43] Zhang G, Bala H, Cheng Y, Shi D, Lv X, Wang P, et al. High efficiency and stable dye-sensitized solar cells with an organic chromophore featuring a binary π -conjugated spacer. *Chem Commun*; 2009:2198–200.
- [44] Hergu e N, Leriche P, Blanchard P, Allain M, Gallego-Planas N, Fr ere P, et al. Evidence for the contribution of sulfur–bromine intramolecular interactions to the self-rigidification of thiophene-based π -conjugated systems. *New J Chem* 2008;32:932–6.
- [45] Prim D, Auffrant A, Plyta ZF, Tranchier JP, Munch FR, Rose E. Bimetallic π -conjugated complexes modulated by a carbonyl spacer: synthesis of arenetricarbonylchromium–ferrocene derivatives. *J Organomet Chem* 2001;624:124–30.
- [46] Becke AD. A new mixing of Hartree-Fock and local density-functional theories. *J Chem Phys* 1993;98:1372–7.
- [47] Lynch BJ, Fast PL, Harris M, Truhlar DG. Adiabatic connection for kinetics. *J Phys Chem A* 2000;104:4811–5.
- [48] Cossi M, Baron V. Time-dependent density functional theory for molecules in liquid solutions. *J Chem Phys* 2001;115:4708–17.
- [49] Frisch MJ, Trucks GW, Schlegel HB, Scuseria GE, Robb MA, Cheeseman JR, et al. Gaussian 03. Revision B05. Pittsburgh PA: Gaussian Inc.; 2003.
- [50] Hara K, Kurashige M, Dan-oh Y, Kasada C, Shinpo A, Arakawa H, et al. Design of new coumarin dyes having thiophene moieties for highly efficient organic-dye-sensitized solar cells. *New J Chem* 2003;27:783–5.
- [51] Hagfeldt A, Gr atzel M. Light-induced redox reactions in nanocrystalline systems. *Chem Rev* 1995;95:49–68.
- [52] Hagberg DP, Marinado T, Karlsson KM, Nonomura K, Hagfeldt A, Sun L, et al. Tuning the HOMO and LUMO energy levels of organic chromophores for dye sensitized solar cells. *J Org Chem* 2007;72:9550–6.